ACS OMEGA

http://pubs.acs.org/journal/acsodf

Article

All-Atom Molecular Dynamics Elucidating Molecular Mechanisms of Single-Transmembrane Model Peptide Dimerization in a Lipid Bilayer

Hayato Itaya, Kota Kasahara,* Qilin Xie, Yoshiaki Yano, Katsumi Matsuzaki, and Takuya Takahashi

Cite This: *ACS Omega* 2021, 6, 11458−11465

Read Online

ACCESS | Metrics & More | Article Recommendations | Supporting Information

ABSTRACT: Protein−protein interactions between transmembrane helices are essential elements for membrane protein structures and functions. To understand the effects of peptide sequences and lipid compositions on these interactions, single-molecule experiments using model systems comprising artificial peptides and membranes have been extensively performed. However, their dynamic behavior at the atomic level remains largely unclear. In this study, we applied the all-atom molecular dynamics (MD) method to simulate the interactions of single-transmembrane helical peptide dimers in membrane environments, which has previously been analyzed by single-molecule experiments. The simulations were performed with two peptides (Ala- and Leu-based artificially designed peptides, termed "host peptide", and the host peptide added with the GXXXG motif, termed "GXXXG peptide"), two membranes (pure-POPC and POPC mixed with 30% cholesterols), and two dimer directions (parallel and antiparallel), consistent with those in the previous experiment. As a result, the MD simulations with parallel dimers reproduced the experimentally observed tendency that introducing cholesterols weakened the interactions in the GXXXG dimer and facilitated those in the host dimer. Our simulation suggested that the host dimer formed hydrogen bonds but the GXXXG dimer did not. However, some discrepancies were also observed between the experiments and simulations. Limitations in the space and time scales of simulations restrict the large-scale undulation and peristaltic motions of the membranes, resulting in differences in lateral pressure profiles. This effect could cause a discrepancy in the rotation angles of helices against the membrane normal.

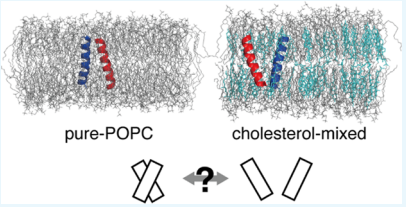

1. INTRODUCTION

Many proteins embedded in biological membranes perform essential functions, such as mediating communications across the membrane and energy synthesis. Elucidating the molecular principles of membrane proteins has gained much attention in the context of molecular biology. In particular, the formation of multimeric complexes in the membrane environment plays an important role to establish the molecular functions of membrane proteins. The characteristics of the protein−protein interactions of membrane proteins are distinct from those of soluble proteins because of the differences in their environments.[1−3] For example, the low permittivity of the membrane environment significantly strengthens the electrostatic interactions compared to the solution environment. Therefore, both the two factors (i) the sequence of the membrane proteins and (ii) the lipid composition of the membrane are essential for protein−protein interactions.

Typically, the protein−protein interactions between membrane proteins are established by the packing of transmembrane helices. The sequences of the binding interface in transmembrane helices have been well characterized; small residues, i.e., Gly, Ala, and Ser, are enriched in the interfaces and tend to be distributed at intervals of two or three residues.[4,5] These kinds of sequence elements are known as motifs, e.g., GXXXG, SXXXG, and GXXXGXXG. The small steric hindrance of these side chains brings the helices closer to each other. In the GXXXG motif, an important example of the transmembrane helix binding motifs, the weak hydrogen bond between the Cα−H and O moieties of Gly residues is considered to be a key player in the binding.[6−10]

Another key feature is the lipid composition of the membrane. The structures and functions of membrane proteins are influenced by lipid composition. In particular, the effects of cholesterol have been well studied. There is much evidence for cholesterol-induced modulations of conformational states, multimer formation, ligand-binding activity, and ion channel activity.[11,12]

To investigate the molecular mechanisms of transmembrane helix binding and the effects of the sequence motif and the membrane composition on their binding, a dimer of single-transmembrane helices can be considered one of the simplest models. Dimerization mechanisms have been extensively studied by targeting stereotypical single-transmembrane

Received: January 26, 2021
Accepted: April 8, 2021
Published: April 22, 2021

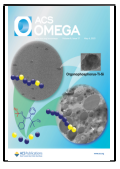

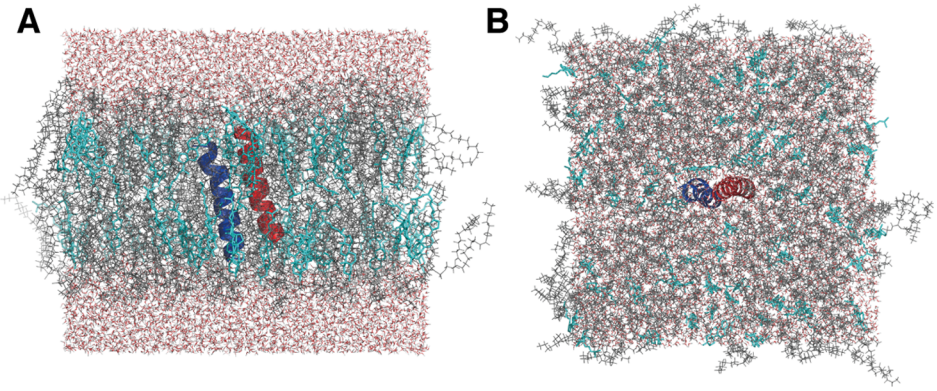

Figure 1. Initial structure of production simulations with the cholesterol-mixed membrane. The gray and cyan lipids are POPCs and cholesterols, respectively. The blue and red ribbons indicate the peptides. The red dots are water molecules. (A) A side view. (B) A top view.

peptides, e.g., glycophorin A[6] and growth hormone receptors.[13,14]

Yano et al.[15−18] reported in vitro binding experiments using single-pair Förster resonance energy transfer (FRET) measurements. These studies analyzed the behavior of model peptides composing a single-transmembrane helix, the sequence of which is a triple repeat of AALALAA and its variant with a GXXXG motif. The single-pair FRET experiments compared the binding kinetics of these peptides in the two types of membrane environments: pure-POPC membrane and a POPC membrane mixed with 30%-cholesterol. Although cholesterols enhanced the binding of the "host" peptide without the GXXXG motif, they inhibited the binding of the GXXXG peptide.[16,17]

The molecular mechanisms of this phenomenon are not fully understood at the atomic level. The atomic details of interactions, such as those in highly complicated, heterogeneous, and dynamical molecular systems, cannot be easily observed through current experimental techniques. A promising method to observe such details is the molecular dynamics (MD) method, which simulates atomic motions of molecular systems based on Newtonian mechanics. Although MD simulations have been extensively applied to investigate the dynamic behavior of membranes and membrane proteins,[19−27] it remains challenging to treat membrane systems. In particular, the success of MD simulations is based on the data from the X-ray crystal structure analyses of proteins. Current MD methods can be efficiently employed for proteins with well-packed, stable folds; however, there are many challenges for their use with unstable proteins with structures that are difficult to be analyzed by experiments, e.g., dynamic features of dimerized transmembrane helices[19] and intrinsically disordered proteins.[20] Further validations of this methodology with direct comparison with experimental observations are required.

Here, we applied the all-atom MD method to analyze molecular systems emulating the in vitro single-pair FRET experiments provided by Yano et al.[16,17] to elucidate the atomic details of transmembrane helices binding with and without the GXXXG motif in the pure-POPC and cholesterol-mixed POPC environments. In addition, we directly compared the results of MD simulations with those of single-pair FRET experiments and discussed the current limitations of MD techniques to provide implications that may improve the simulation method.

2. RESULTS

2.1. Simulation Overview. We analyzed molecular systems comprising a dimer of a single-transmembrane peptide embedded in a membrane surrounded by explicit water molecules. For the single-transmembrane peptide, two types of sequences were used: AALALAA-AALALAA-AALALAA and AALALAA-AGLALGA-AALALAA. The first sequence is the triple repeat of AALALAA. The second introduces the GXXXG motif in the middle of the first sequence to enhance the dimerization. In this paper, we termed these model peptides host peptide and GXXXG peptide, respectively, hereinafter. To eliminate the charges at the termini, the model peptides were capped with standard capping groups in the following manner: an acetyl group at the N-terminus and a methyl group at the C-terminus. For the membrane, two types of lipid bilayers were used: a pure-POPC bilayer and a bilayer with 30% cholesterol and 70% POPC (the percentage indicates the ratio of the number of lipid molecules). The 30% cholesterol mimics the cholesterol composition of the plasma membrane.[21] Additionally, the pure-POPC membrane mimics intracellular membranes, such as the endoplasmic reticulum. For simplicity, we termed these membrane models pure-POPC membrane and cholesterol-mixed membrane, respectively, hereinafter.

In total, eight systems were analyzed: the combination of two peptide sequences (host and GXXXG peptides), two dimer orientations (parallel and antiparallel), and two membranes (pure-POPC and cholesterol mixed). For each system, four runs of 500 ns NPT simulations were performed with different initial atomic velocities. The trajectories of the last 300 ns in each run were analyzed. The simulation model is shown in Figure 1. The simulation conditions are summarized in Table S1 in the Supporting Information.

2.2. Conformational Stability during the Simulation. In all of the simulation conditions, transmembrane peptides retained their helical conformation, except for few residues at the termini, and no irreversible rupture of the membrane was observed (Figures S1 and S2 in the Supporting Information). The root-mean-square fluctuation (RMSF) showed that there were no significant conformational changes in each peptide in the simulations, whereas their termini tended to fluctuate (Figure S3 in the Supporting Information). These results imply that the initial conformations were reasonably stable during the entire simulations.

Comparing the host and GXXXG peptides, replacing Ala with Gly at residues 9 and 13 increased the flexibility of the

https://doi.org/10.1021/acsomega.1c00482
ACS Omega 2021, 6, 11458−11465

peptide backbone (Figure S4 in the Supporting Information), but the average values of the dihedral angles did not change significantly. In addition, the N-terminal region of the host peptide was unstable compared with that of the GXXXG peptide (Figure S3 in the Supporting Information), although these two peptides have the same initial structures.

Note that each trajectory may not reach equilibrium in the 500 ns time course. There are detectable differences among the four replicates of simulations with different initial velocities (and different initial positions of cholesterols). We primarily focus on the differences in averaged trends over four repeated runs rather than the details of each trajectory.

2.3. Peptide−Peptide Contacts. To assess the interactions between two transmembrane peptides, the intermolecular, inter-residue contacts were detected based on the criterion that the Cα−Cα distance is within 8.0 Å. For the dimers with a parallel orientation, the average numbers (and the standard errors) of the inter-residue contacts between the GXXXG peptides were 23.5 (7.66) and 4.64 (2.53) for pure-POPC and cholesterol-mixed membranes, respectively, and for the host peptide, these values were 10.44 (3.96) and 8.30 (2.59), respectively (Table S1 in the Supporting Information). The GXXXG peptide was in tighter contact than the host peptides in the pure-POPC environment (Figure 2), reflecting

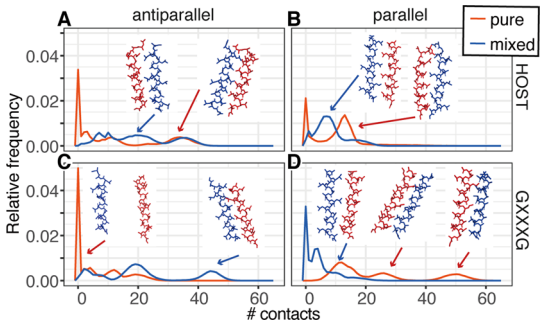

Figure 2. Distributions of the number of contacts in each condition. The horizontal axis indicates the number of inter-residue contacts between two peptides. The vertical axis is the relative frequency in each ensemble. The upper row (A and B) and the lower row (C and D) show the host and GXXXG peptides, respectively. The left column (A and C) and right column (B and D) show the antiparallel and parallel directions of the dimer, respectively. The red and blue curves correspond to pure-POPC and cholesterol-mixed membrane, respectively. The bin width of the histogram is 1.

the fact that the GXXXG motif facilitates the dimer formation. The host peptide in the pure-POPC membrane yielded a bimodal distribution (Figure 2B, red). The first peak at zero number of contacts indicates that the dimer was dissociated. For the GXXXG peptide in the pure-POPC membrane, the dimer was not dissociated, and there were peaks around 11, 26, and 50 contacts (Figure 2D, red). The snapshots of the third peak show tightly contacted dimer conformations that are not observed for the host peptides (Figure 2D). In addition, it was confirmed that adding cholesterols to the membrane clearly reduced the interactions of the GXXXG dimers. The contact distribution for the GXXXG peptide in the cholesterol-mixed membrane has a strong peak at zero contact. These results were qualitatively consistent with those of the single-pair FRET experiments reported by Yano et al.[17]

In the antiparallel configuration, cholesterol facilitated interactions of the host peptide dimer (Figure 2A), in agreement with the findings of Yano et al.[16] In contrast, the results of the antiparallel GXXXG dimer disagreed with the experimental results. Although the experiment reported that the GXXXG helix dimerization was inhibited by addition of cholesterols in both parallel and antiparallel configurations,[17] our simulation with the antiparallel GXXXG dimer yielded more frequent contact in the cholesterol-mixed membrane than in the pure-POPC membrane.

2.4. Hydrogen Bonds. The binding of the two transmembrane helices included several hydrogen bonds. The hydrogen bonds were assessed using the criteria that the acceptor−donor distance was less than or equal to 3.5 Å, and the donor−hydrogen−acceptor angle was greater than or equal to 120°. We analyzed the two types of hydrogen bonds: standard backbone hydrogen bonds (N−H···O) and weak hydrogen bonds (Cα−H···O). As a result, in the parallel configuration, the dimer in the cholesterol-mixed membrane exhibited fewer hydrogen bonds than those in the pure-POPC membrane for both the peptides (Figure 3C,D). Interestingly,

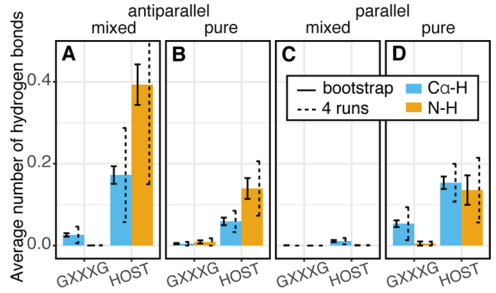

Figure 3. Average number of hydrogen bonds between the two peptides under each condition. (A and C) and (B and D) show the data for cholesterol-mixed and pure-POPC membranes, respectively. (A and B) and (C and D) present the antiparallel and parallel directions of the dimer, respectively. Cyan and orange indicate Cα−H··· O and N−H···O hydrogen bonds, respectively. The error bars shown as the dashed lines indicate the standard errors calculated over the four trajectories. Those shown in solid lines represent the standard errors calculated by performing bootstrap analysis. In this analysis, a random sampling of a trajectory with replacement from the four trajectories was repeated four times, and an ensemble with the same number of snapshots as the original ensemble was generated. The standard errors were calculated over 100 regenerated ensembles.

the antiparallel configuration showed the opposite trend (Figure 3A,B). This is consistent with the differences in the number of inter-residue contacts shown in Figure 2. Comparing the host and GXXXG peptides, a lower frequency of hydrogen bond formation was observed in the GXXXG peptide than in the host peptide, regardless of the frequency of inter-residue contacts. In the parallel direction, although the GXXXG peptide had more frequent inter-residue contacts, it had fewer hydrogen bonds than the host peptide. This indicates that the GXXXG motif facilitates the peptide−peptide binding but it decreases hydrogen bonding and these binding modes are distinct between the host and GXXXG peptide dimers. Hydrogen bonds were not major driving forces for the dimerization of the GXXXG peptides. The hydrogen bonds in the host peptides were formed at the termini (Figure S5 in the Supporting Information).

2.5. Helix Tilt Angles and Membrane Thickness. The binding modes of peptide dimers can also be analyzed in terms of the tilt angles and crossing angles of the two helices (Figures

https://doi.org/10.1021/acsomega.1c00482
ACS Omega 2021, 6, 11458−11465

4 and S6 in the Supporting Information). The tilt angle is defined as the angle between the membrane normal and the

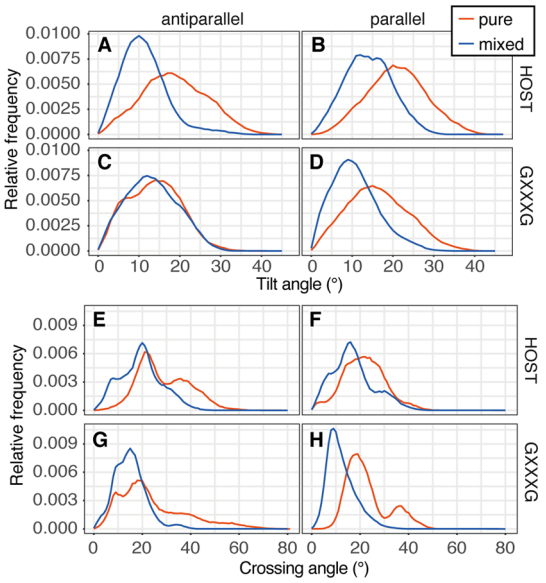

Figure 4. Distributions of tilt (A–D) and crossing (E–H) angles. Red and blue lines indicate results of pure-POPC and cholesterol-mixed membranes, respectively. The bin width of the histogram is 0.1. The panels (A, B, E, and F) and (C, D, G, and H) show the host and GXXXG peptides, respectively. The left column (A, C, E, and G) and the right column (B, D, F, and H) show the antiparallel and parallel directions of the dimer, respectively.

vector sum of the helical axes of the two peptides. The crossing angle is the angle between the two helical axes. In general, the host peptides had larger angles than the GXXXG peptide, and the pure-POPC membrane exhibited larger angles than the cholesterol-mixed membrane.

To some extent, the effects of the membrane environment on the angles can be explained in terms of membrane thickness. Embedding the cholesterols into the POPC membrane thickened the membrane, but the sequence and direction of the peptide dimer (parallel or antiparallel) did not affect the membrane thickness (Figure 5), which is consistent

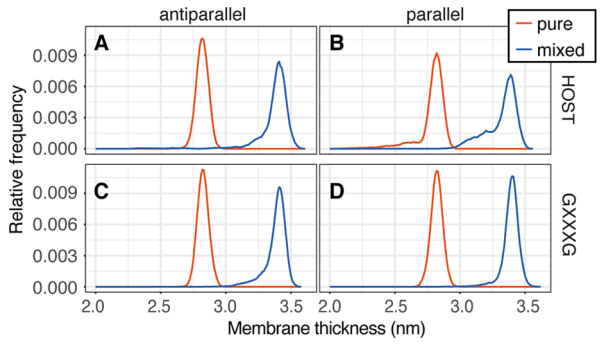

Figure 5. Distributions of the membrane thickness. Red and blue lines indicate the results of pure-POPC and cholesterol-mixed membranes, respectively. The membrane thickness was measured as the distance between the centroids of carbonyl oxygen atoms in each leaflet. The upper row (A and B) and the lower row (C and D) show the host and GXXXG peptides, respectively. The left column (A and C) and the right column (B and D) show the antiparallel and parallel directions of the dimer, respectively. The bin width of the histogram is 0.1.

with the findings of the previous experiment.[16] Insertion of stiff lipids, that is, cholesterol, caused ordering of the acyl chains of POPC and thickening of the membrane (Figure S7 in the Supporting Information). Thinner membranes tended to have larger transmembrane helix angles because of the hydrophobic mismatch.[22] Tilted conformations can minimize the hydrophobic mismatch when the membrane is thinner than the length of the helices.

In contrast, larger angles of the host dimer than the GXXXG dimer were not caused by the hydrophobic mismatch because the membrane thickness did not depend on the peptide species or direction. As mentioned above, these two types of transmembrane helices had different mechanisms of dimerization; the GXXXG dimer had tight inter-residue contacts, whereas the host dimer had some hydrogen bonds. This difference can cause differences in the angles. To form a tight packing of the dimer interface, there is a steric requirement to maximize inter-residue contacts between the two helices. Crossing angles that are too large decrease the contacts between the terminal sides of the helices, and crossing angles that are too small may involve Leu–Leu side chain crashes, creating a distance between the helices. Therefore, the host peptides that have some intermolecular hydrogen bonds allow larger angles compared with the GXXXG peptides.

2.6. Peptide–Lipid Interactions. The effects of lipid composition on the peptide–peptide interactions can be categorized into two classes: direct and indirect effects. As an example of indirect effects, the cholesterol-mixed membrane was thicker and affected the peptide–peptide interactions by adjusting the hydrophobic thickness. In contrast, the direct effects are mediated by direct contact or interaction between peptide and lipid molecules. To assess the direct effects, we analyzed the duration times for a peptide–lipid interaction, which is defined by the following criterion: the minimum distance between the Cα of peptides and the representative head group atom of a lipid molecule (P for POPC and O for cholesterol) is less than or equal to 10 Å. The time from peptide–lipid association to their dissociation was measured for every association/dissociation event. As a result, although there were detectable differences in the duration times between POPC and cholesterol, the difference was not large (Figure 6).

3. DISCUSSIONS

3.1. Convergence of Simulation Trajectories. In this study, four repeats of 500 ns simulations were performed for each condition. We confirmed that the peptide conformation was stably maintained for 500 ns in all of the simulations (Figure S1 in the Supporting Information). However, the interactions between the two peptides diverged during the simulation (Figure S8 in the Supporting Information). The distribution of the number of interpeptide contacts significantly differed among the four trajectories under the same condition (Figure S9 in the Supporting Information). In general, because of the complexity of the membrane protein system, an equilibrium state cannot be easily achieved in a single run of canonical MD simulations.[23]

However, a comparison of ensemble averages over the last 200 ns of the four trajectories yielded remarkable differences among the different conditions. While the distribution of interpeptide contacts in each 200 ns time window shows detectable differences between 200–400 and 300–500 ns (Figure S10 in the Supporting Information), the differences among the conditions were qualitatively conserved. We

https://doi.org/10.1021/acsomega.1c00482
ACS Omega 2021, 6, 11458–11465

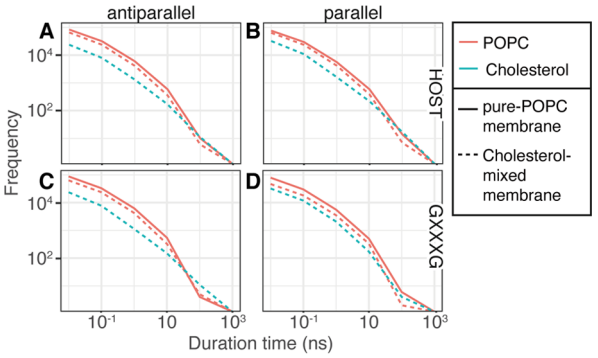

Figure 6. Distribution of duration times for the event beginning with a lipid molecule encountering the peptide and ending with the dissociation. The horizontal axis means the duration time, and the vertical axis means the observed number of events. Solid and dashed lines indicate the results from the simulations with pure-POPC and cholesterol-mixed membranes, respectively. Color specifies species of lipid molecules: orange for POPC and cyan for cholesterol. The upper row (A and B) and the lower row (C and D) show the host and GXXXG peptides, respectively. The left column (A and C) and the right column (B and D) show the antiparallel and parallel directions of the dimer, respectively.

assessed errors for the average number of interpeptide contacts (Figure S11 in the Supporting Information) and hydrogen bonds (Figure 3) in the following two ways: the standard errors calculated over the four samples of trajectory and those calculated with bootstrap analysis. The values showed marked differences among the conditions of the lipid composition, sequence motif, and dimer orientation.

3.2. Facilitation of Dimer Formation by the GXXXG Motif. The GXXXG motif is a well-known sequence element that enhances the homodimerization of transmembrane helices.[24] As a prominent example, glycophorin A contains the GXXXG motif, and it has been reported that the three-dimensional structure of its dimer forms an hourglass-shaped dimer (a helix−helix crossing angle of ∼40°) with Cα−H weak hydrogen bonds between Gly residues.[6−8] In contrast, our simulation with the GXXXG motif revealed a tightly packed dimer with a small crossing angle (Figure 4), in agreement with the findings of the single-pair FRET experiments.[17] In addition, only a few hydrogen bonds were observed in the GXXXG dimer (Figure 3). This difference in the mechanisms of dimerization by the GXXXG motif is likely caused by the peptide sequences. Statistically, β-branched residues such as Val and Ile are enriched at the neighboring position of Gly of the GXXXG motif, like glycophorin A[25] and ErbB growth factor receptors. Our model peptides have two Leu residues, which have a γ-branched side chain with a large variety of rotamers, between two Gly residues. Entropy loss involved in the binding of these Leu residues can impact the binding mechanism of the GXXXG dimer. In addition, our model peptides consist of only three types of residues, Gly, Ala, and Leu, and the simple pattern of this sequence makes it possible to form tight packing of the entire length of the two helices. Introducing the Gly residue into the host peptide increases the flexibility of the helical backbone (Figure S4)[26] and allows dimer packing to be optimized.

3.3. Effects of Cholesterols in the Membrane on the Dimerization of the Host Peptides. For the host peptide, the single-pair FRET experiments by Yano et al.[16] showed that the dimer formation was observed in the antiparallel dimer in the cholesterol-mixed membrane, and no FRET signals were observed in the other three conditions, namely, the antiparallel dimer in the pure-POPC and the parallel dimer in both the membrane conditions. This indicates that cholesterol enhances the dimerization of the host helix, but the dimer cannot be formed in the parallel configuration. Our previous in vitro studies showed that the helix macrodipole is an essential factor for antiparallel dimerization of the host peptides.[15,16,18] The association enthalpy of the host helix antiparallel dimer coincided with the estimated energy of the helix macrodipole.[18] In general, whereas the helix macrodipole effect is strongly shielded in high permittivity environments, burying the helix termini into the membrane environment reduces the shielding effects of the solvent. A theoretical study by Sengupta et al.[27] reported that shorter helices yield stronger helix macrodipole effects. Our simulations reproduced an increase in peptide−peptide interactions in the antiparallel dimers by introducing cholesterol (Figure 2A). Although a certain amount of interpeptide contacts were observed in the parallel dimers (Figure 2B), they were clearly weaker than those of the antiparallel dimer in the cholesterol-mixed membrane.

However, there is a discrepancy between the experiments and simulations regarding the tendencies of the helix tilt and crossing angles. The experiments indicated that the helix orientation angles were almost vertical (∼0°) in the pure-POPC and ∼28° in the cholesterol-mixed membrane.[16] Note that the orientation angles measured in the experiments are calculated from the amide I bonds, and the helix tilt angles against the membrane normal and crossing angles cannot be distinguished. Our simulations yielded more tilted dimer conformations in the pure-POPC membrane (crossing angles of ∼20° in the cholesterol-mixed membrane and ∼29° in the pure-POPC membrane for the crossing angles). According to the results of helix orientation angles, Yano et al. concluded that the host helices form an hourglass-shaped dimer with the penetration of water molecules into the membrane regions to release the lateral pressure in the cholesterol-mixed membrane. Our MD simulation may not precisely reproduce the macro properties of the membrane environment, including the lateral pressure, owing to the limited size of the simulation cell, and thus the dimer did not form the hourglass shape. Instead, the dimer was close to a vertical orientation to reduce the hydrophobic mismatch, given that the membrane was thickened by the addition of cholesterols. An increase in the interpeptide contacts was driven by strengthening helix macrodipole interactions by thickening the membrane.

As discussed in the study by Yano et al.,[16] there are three driving forces for the dimerization in the cholesterol-mixed membrane: (i) release of the lateral pressure by dimerization, (ii) lipophobic interactions, and (iii) strengthening of the helix macrodipole interactions. Our simulations may not adequately account for effect (i). To assess effect (ii), we analyzed duration times for the events in which a lipid molecule interacts with the peptide dimer (Figure 6) and found that there was no notable difference in the kinetics of lipid−peptide interactions between the pure-POPC and cholesterol-mixed membranes. This result is not paradoxical to that of the experiments by Yano et al. Effect (iii) facilitated the dimer formation in the simulations.

3.4. Effects of Cholesterols in the Membrane on the Dimerization of the GXXXG Peptides. In the models of the GXXXG parallel dimers, our simulations showed that introducing cholesterols reduced the interpeptide contacts,

https://doi.org/10.1021/acsomega.1c00482
ACS Omega 2021, 6, 11458−11465

which agrees with the results of the single-pair FRET experiments.[17] Because the cholesterols thickened the membrane (Figure 5), the tilt and crossing angles decreased to minimize the hydrophobic mismatch (Figure 4). Tighter packing of the two helices sterically requires a certain crossing angle, and thus a decrease in the crossing angle weakens the peptide−peptide packing.

In contrast, the behavior of the GXXXG antiparallel dimer did not agree with the experimental results, which reported that cholesterols inhibit the dimer formation of the GXXXG peptides. Our simulations showed that the GXXXG helices had a certain amount of interpeptide contacts, even in the cholesterol-mixed membrane (Figure 2C). The introduction of cholesterols increased the membrane thickness (Figure 4) and decreased the angles (Figure 3), but interactions were retained, in contrast to the parallel dimer. This discrepancy may originate from the differences in the treatment of lateral pressure. Yano et al.[17] discussed that it is difficult to release lateral pressure for the GXXXG peptides because of the flexibility of the Gly backbone and this effect can inhibit dimerization by cholesterol. Our simulation may not appropriately reproduce the macro properties of the membrane.

4. CONCLUSIONS

We investigated the molecular mechanisms of dimer formation in single-transmembrane model peptides using all-atom MD simulations. To compare our simulations with the in vitro experiments reported by Yano et al.[16,17] directly, we performed simulations using a combination of the various conditions: two types of peptide sequences (the host and GXXXG peptides), two types of dimer topology (parallel and antiparallel), and two types of membrane composition (the pure-POPC and cholesterol-mixed membranes). In the same conditions, the simulations reproduced the trends observed in the experiments. Introducing cholesterols facilitated the dimer formation of the host peptides and inhibited the formation of the GXXXG dimer in the parallel configuration.

In contrast, there are some discrepancies between the MD simulations and the in vitro experiments by Yano et al.[16,17] Several features that are difficult to include adequately in MD simulations. (i) Owing to the limitation of the simulation cell size and applying the periodic boundary condition, the macroscopic mechanical properties of the membrane may not be reproduced by MD simulations. The wavelength of the undulation and peristaltic motion of the membrane is limited up to the cell dimension along the lateral direction.[28,29] To discuss the impacts of such effects, further evaluations using molecular models with different cell sizes should be performed elsewhere. (ii) The simulations may not capture equilibrium properties because of the limitation of the time scale.[23] To reduce the bias from the initial condition, we repeated four simulation runs with different initial atomic velocities (and different positions of cholesterols) for each system. To improve the reliability of sampling for equilibrium states, generalized ensemble methods represent a promising approach. Sampling the canonical ensemble by exploring the conformational space and by conducting analyses of the free-energy landscape provide insights into the binding mode of dimer formation. Additionally, information on the interaction energy for dimerization can be dissected based on the conformational ensemble including both the associated and dissociated states. However, the application of generalized ensemble approaches to membrane systems is not necessarily straightforward.[19,30,31] Further developments of the method are necessary.

The simulation study dissects the physical features that are intrinsically inseparable in experiments, namely, local molecular interactions and macroscopic mechanical features of the membrane. For example, the result of the dimer formation of the antiparallel GXXXG helices being inhibited by cholesterols could not be reproduced by our simulations, implying that the effects omitted in the simulations would be important for this phenomenon. In contrast, the local interactions treated in the simulations may be sufficient to explain the cholesterol-induced inhibition of the parallel dimers. There are essential differences between parallel and antiparallel dimers.

5. METHODS

5.1. Simulation System. For the initial structures of MD simulations, two types of dimer conformations, which are parallel and antiparallel dimers, were built by the template-based modeling based on the bacteriorhodopsin structure (PDB ID: 2ntu) using MODELLER software.[32] The template was arbitrarily selected as a typical structure of the transmembrane helix bundle without any specific motif. The template of the parallel dimer was the first helix (residues 8−28) and the seventh helix (residues 202−222), whereas that of the antiparallel dimer was the sixth helix (residues 168−188) and the seventh helix (residues 202−222). The dimer models were embedded in a lipid bilayer and bathed in a 0.15 M NaCl solution using CHARMM-GUI.[33] The membrane comprised 256 lipid molecules (128 lipids for each leaflet). The cell dimensions were approximately 90 Å × 90 Å × 70 Å in the initial structure.

In total, eight systems were analyzed: the combination of two peptide sequences, two dimer orientations, and two membranes. These models were prepared to emulate the experiments by Yano et al.[16,17] For each of the eight models, we ran four series of simulations independently. The initial configuration of the cholesterol molecules and initial atomic velocities were generated by different random seeds for each run. The simulation conditions are summarized in Table S1.

5.2. Molecular Simulation Methods. The equilibration protocol used the default setting of CHARMM-GUI. First, the energy minimization was performed using the steepest descent method. Second, the NPT simulations with a Berendsen barostat were performed with the positional restraint; the force constant of which was gradually relaxed. Subsequently, a 500 ps NPT simulation was performed without restraint. The integration time step for the equilibration was 2.0 fs, and the covalent bonds with hydrogen atoms were constrained by the LINCS method.[34,35] Finally, 500 ns NPT simulations were performed at 298 K and 1.0 atm using the Nosé−Hoover thermostat and the Parrinello−Rahman barostat with a 2.0 fs integration time step. In total, 16 μs simulations were performed. The trajectory for the last 300 ns of each run was analyzed. The CHARMM36m force field[36] and the TIP3P water model[37] were applied. Electrostatic potentials were calculated using the smooth particle mesh Ewald method.[38] The real-space cutoff length was 1.0 nm. All of the simulations were performed using GROMACS software.[39]

https://doi.org/10.1021/acsomega.1c00482
ACS Omega 2021, 6, 11458−11465

ASSOCIATED CONTENT

Supporting Information

The Supporting Information is available free of charge at https://pubs.acs.org/doi/10.1021/acsomega.1c00482.

Time evolution of helix content of each run (Figure S1); examples of snapshots at the final steps (Figure S2); RMSF and helix content of each residue (Figure S3); backbone dihedral angles of the 9th and 13th residues (Figure S4); residue-wise frequency for hydrogen bond formation (Figure S5); distributions of helix tilt angles (Figure S6); order parameters of POPC (Figure S7); time evolution of the number of interpeptide contacts (Figure S8); distribution of the number of interpeptide contacts in each replicate of simulations (Figure S9); distribution of the number of interpeptide contacts in each 200 ns time window (Figure S10); average and errors for the number of inter-residue contacts (Figure S11); and summary of simulation systems (Table S1) (PDF)

AUTHOR INFORMATION

Corresponding Author

Kota Kasahara − *College of Life Sciences, Ritsumeikan University, Kusatsu, Shiga 525-8577, Japan;* orcid.org/0000-0003-0207-6271; Email: ktkshr@fc.ritsumei.ac.jp

Authors

Hayato Itaya − *Graduate School of Life Sciences, Ritsumeikan University, Kusatsu, Shiga 525-8577, Japan*

Qilin Xie − *College of Pharmaceutical Sciences, Ritsumeikan University, Kusatsu, Shiga 525-8577, Japan*

Yoshiaki Yano − *Graduate School of Pharmaceutical Sciences, Kyoto University, Kyoto 606-8501, Japan*

Katsumi Matsuzaki − *Graduate School of Pharmaceutical Sciences, Kyoto University, Kyoto 606-8501, Japan;* orcid.org/0000-0002-0182-1690

Takuya Takahashi − *College of Life Sciences, Ritsumeikan University, Kusatsu, Shiga 525-8577, Japan*

Complete contact information is available at: https://pubs.acs.org/10.1021/acsomega.1c00482

Author Contributions

The manuscript was written through contributions of all authors. All authors have given approval to the final version of the manuscript.

Funding

K.K. was supported by JSPS KAKENHI Grant Number JP20K12069.

Notes

The authors declare no competing financial interest.

ACKNOWLEDGMENTS

The computational resources were provided by the HPCI System Research Project (Project IDs: hp190017, hp190018, hp200063, and hp200090), the NIG supercomputer at ROIS National Institute of Genetics, Human Genome Center (the University of Tokyo), and Research Center for Computational Science, Okazaki, Japan.

REFERENCES

(1) Lee, A. G. How lipids affect the activities of integral membrane proteins. *Biochim. Biophys. Acta, Biomembr.* **2004**, *1666*, 62−87.

(2) Marsh, D. Protein modulation of lipids, and vice-versa, in membranes. *Biochim. Biophys. Acta, Biomembr.* **2008**, *1778*, 1545−1575.

(3) Phillips, R.; Ursell, T.; Wiggins, P.; Sens, P. Emerging roles for lipids in shaping membrane-protein function. *Nature* **2009**, *459*, 379−385.

(4) Russ, W. P.; Engelman, D. M. The GxxxG motif: A framework for transmembrane helix-helix association. *J. Mol. Biol.* **2000**, *296*, 911−919.

(5) Feng, X.; Barth, P. A topological and conformational stability alphabet for multipass membrane proteins. *Nat. Chem. Biol.* **2016**, *12*, 167−173.

(6) Smith, S. O.; Song, D.; Shekar, S.; Groesbeek, M.; Ziliox, M.; Aimoto, S. Structure of the Transmembrane Dimer Interface of Glycophorin A in Membrane Bilayers†. *Biochemistry* **2001**, *40*, 6553−6558.

(7) Senes, A.; Ubarretxena-Belandia, I.; Engelman, D. M. The Cα—H···O hydrogen bond: A determinant of stability and specificity in transmembrane helix interactions. *Proc. Natl. Acad. Sci. U.S.A.* **2001**, *98*, 9056−9061.

(8) Arbely, E.; Arkin, I. T. Experimental Measurement of the Strength of a Cα−H···O Bond in a Lipid Bilayer. *J. Am. Chem. Soc.* **2004**, *126*, 5362−5363.

(9) Mueller, B. K.; Subramaniam, S.; Senes, A. A frequent, GxxxG-mediated, transmembrane association motif is optimized for the formation of interhelical Cα−H hydrogen bonds. *Proc. Natl. Acad. Sci. U.S.A.* **2014**, *111*, E888−E895.

(10) Anderson, S. M.; Mueller, B. K.; Lange, E. J.; Senes, A. Combination of Cα−H Hydrogen Bonds and van der Waals Packing Modulates the Stability of GxxxG-Mediated Dimers in Membranes. *J. Am. Chem. Soc.* **2017**, *139*, 15774−15783.

(11) Baenziger, J. E.; Morris, M. L.; Darsaut, T. E.; Ryan, S. E. Effect of membrane lipid composition on the conformational equilibria of the nicotinic acetylcholine receptor. *J. Biol. Chem.* **2000**, *275*, 777−784.

(12) Corradi, V.; Sejdiu, B. I.; Mesa-Galloso, H.; Abdizadeh, H.; Noskov, S. Y.; Marrink, S. J.; Tieleman, D. P. Emerging Diversity in Lipid−Protein Interactions. *Chem. Rev.* **2019**, *119*, 5775−5848.

(13) Prakash, A.; Janosi, L.; Doxastakis, M. GxxxG Motifs, Phenylalanine, and Cholesterol Guide the Self-Association of Transmembrane Domains of ErbB2 Receptors. *Biophys. J.* **2011**, *101*, 1949−1958.

(14) Brooks, A. J.; Dai, W.; O'Mara, M. L.; Abankwa, D.; Chhabra, Y.; Pelekanos, R. A.; Gardon, O.; Tunny, K. A.; Blucher, K. M.; Morton, C. J.; et al. Mechanism of Activation of Protein Kinase JAK2 by the Growth Hormone Receptor. *Science* **2014**, *344*, No. 1249783.

(15) Yano, Y.; Matsuzaki, K. Measurement of Thermodynamic Parameters for Hydrophobic Mismatch 1: Self-Association of a Transmembrane Helix. *Biochemistry* **2006**, *45*, 3370−3378.

(16) Yano, Y.; Kondo, K.; Kitani, R.; Yamamoto, A.; Matsuzaki, K. Cholesterol-Induced Lipophobic Interaction between Transmembrane Helices Using Ensemble and Single-Molecule Fluorescence Resonance Energy Transfer. *Biochemistry* **2015**, *54*, 1371−1379.

(17) Yano, Y.; Kondo, K.; Watanabe, Y.; Zhang, T. O.; Ho, J.-J.; Oishi, S.; Fujii, N.; Zanni, M. T.; Matsuzaki, K. GXXXG-Mediated Parallel and Antiparallel Dimerization of Transmembrane Helices and Its Inhibition by Cholesterol: Single-Pair FRET and 2D IR Studies. *Angew. Chem.* **2017**, *129*, 1782−1785.

(18) Yano, Y.; Watanabe, Y.; Matsuzaki, K. Thermodynamic and kinetic stabilities of transmembrane helix bundles as revealed by single-pair FRET analysis: Effects of the number of membrane-spanning segments and cholesterol. *Biochim. Biophys. Acta, Biomembr.* **2021**, *1863*, No. 183532.

(19) Kharche, S. A.; Sengupta, D. Dynamic protein interfaces and conformational landscapes of membrane protein complexes. *Curr. Opin. Struct. Biol.* **2020**, *61*, 191−197.

(20) Kasahara, K.; Terazawa, H.; Takahashi, T.; Higo, J. Studies on Molecular Dynamics of Intrinsically Disordered Proteins and Their Fuzzy Complexes: A Mini-Review. *Comput. Struct. Biotechnol. J.* **2019**, *17*, 712−720.
(21) Song, Y.; Kenworthy, A. K.; Sanders, C. R. Cholesterol as a co-solvent and a ligand for membrane proteins. *Protein Sci.* **2014**, *23*, 1−22.
(22) Ren, J.; Lew, S.; Wang, Z.; London, E. Transmembrane orientation of hydrophobic alpha-helices is regulated both by the relationship of helix length to bilayer thickness and by the cholesterol concentration. *Biochemistry* **1997**, *36*, 10213−10220.
(23) Dynamics of Lipids, Cholesterol, and Transmembrane α-Helices from Microsecond Molecular Dynamics Simulations. *J. Phys. Chem. B* **2014**, *118* 13590 13600. DOI: 10.1021/jp507027t.
(24) Teese, M. G.; Langosch, D. Role of GxxxG Motifs in Transmembrane Domain Interactions. *Biochemistry* **2015**, *54*, 5125−5135.
(25) Senes, A.; Gerstein, M.; Engelman, D. M. Statistical analysis of amino acid patterns in transmembrane helices: the GxxxG motif occurs frequently and in association with β-branched residues at neighboring positions. *J. Mol. Biol.* **2000**, *296*, 921−936.
(26) Högel, P.; Götz, A.; Kuhne, F.; Ebert, M.; Stelzer, W.; Rand, K. D.; Scharnagl, C.; Langosch, D. Glycine Perturbs Local and Global Conformational Flexibility of a Transmembrane Helix. *Biochemistry* **2018**, *57*, 1326−1337.
(27) Sengupta, D.; Behera, R. N.; Smith, J. C.; Ullmann, G. M. The alpha helix dipole: screened out? *Structure* **2005**, *13*, 849−855.
(28) Lindahl, E.; Edholm, O. Mesoscopic Undulations and Thickness Fluctuations in Lipid Bilayers from Molecular Dynamics Simulations. *Biophys. J.* **2000**, *79*, 426−433.
(29) Braun, A. R.; Brandt, E. G.; Edholm, O.; Nagle, J. F.; Sachs, J. N. Determination of Electron Density Profiles and Area from Simulations of Undulating Membranes. *Biophys. J.* **2011**, *100*, 2112−2120.
(30) Mori, T.; Miyashita, N.; Im, W.; Feig, M.; Sugita, Y. Molecular dynamics simulations of biological membranes and membrane proteins using enhanced conformational sampling algorithms. *Biochim. Biophys. Acta, Biomembr.* **2016**, *1858*, 1635−1651.
(31) Rajagopal, N.; Nangia, S. Obtaining Protein Association Energy Landscape for Integral Membrane Proteins. *J. Chem. Theory Comput.* **2019**, *15*, 6444−6455.
(32) Webb, B.; Sali, A. Comparative Protein Structure Modeling Using MODELLER. *Curr. Protoc. Bioinf.* **2016**, *54*, 5.6.1−5.6.37.
(33) Jo, S.; Cheng, X.; Lee, J.; Kim, S.; Park, S. J.; Patel, D. S.; Beaven, A. H.; Lee, K. I.; Rui, H.; Park, S.; et al. CHARMM-GUI 10 years for biomolecular modeling and simulation. *J. Comput. Chem.* **2017**, *38*, 1114−1124.
(34) Hess, B.; Bekker, H.; Berendsen, H. J. C.; Fraaije, J. G. E. M. LINCS: a linear constraint solver for molecular simulations. *J. Comput. Chem.* **1997**, *18*, 1463−1472.
(35) Hess, B. P-LINCS: A Parallel Linear Constraint Solver for Molecular Simulation. *J. Chem. Theory Comput.* **2008**, *4*, 116−122.
(36) Huang, J.; Rauscher, S.; Nawrocki, G.; Ran, T.; Feig, M.; de Groot, B. L.; Grubmüller, H.; Mackerell, A. D. CHARMM36m: an improved force field for folded and intrinsically disordered proteins. *Nat. Methods* **2017**, *14*, 71−73.
(37) Jorgensen, W. L.; Chandrasekhar, J.; Madura, J. D.; Impey, R. W.; Klein, M. L. Comparison of simple potential functions for simulating liquid water. *J. Chem. Phys.* **1983**, *79*, 926−935.
(38) Essmann, U.; Perera, L.; Berkowitz, M. L.; Darden, T.; Lee, H.; Pedersen, L. G. A smooth particle mesh Ewald method. *J. Chem. Phys.* **1995**, *103*, 8577−8593.
(39) Abraham, M. J.; Murtola, T.; Schulz, R.; Páll, S.; Smith, J. C.; Hess, B.; Lindahl, E. GROMACS: High performance molecular simulations through multi-level parallelism from laptops to supercomputers. *SoftwareX* **2015**, *1−2*, 19−25.

https://doi.org/10.1021/acsomega.1c00482
ACS Omega 2021, 6, 11458−11465